Thermal Separation: Interplay between the Soret Effect and Entropic Force Gradient

Yusuke T. Maeda,[1] Axel Buguin,[2] and Albert Libchaber[1]

[1]*Center for Studies in Physics and Biology, The Rockefeller University, New York, New York 10021, USA*
[2]*Institut Curie, Centre de recherche, CNRS/UMR, Paris 75248, France*

(Received 13 December 2010; revised manuscript received 11 April 2011; published 11 July 2011)

Thermophoresis, the Soret effect, depletes a high concentration of a polyethylene glycol polymer solution from the hot region and builds a concentration gradient. In such a solution, solutes of small concentration experience thermophoresis and polyethylene glycol concentration-dependent restoring forces. We report that by using focused laser heating and varying the polyethylene glycol concentration one observes geometrical localizations of solutes like DNA and RNA into patterns such as a ring. For DNA up to 5.6 kbp, the ring size decreases following a behavior analogous to a gel electrophoresis separation. Above 5.6 kbp, the ring diameter increases with the DNA length. Mixtures of DNA and RNA can be separated as well as different RNA lengths. Separation of colloids is also observed. The experiments might be relevant for the separation of small RNA ribozymes in an early stage of life.

DOI: 10.1103/PhysRevLett.107.038301 PACS numbers: 82.70.Dd, 66.10.C−, 82.60.Lf, 87.14.G−

Introduction.—A suspension bombarded by water molecules, the solute, experiences random instantaneous forces but a zero average force. But in a temperature gradient, with the solute at rest, a suspension will move with a velocity proportional to the temperature gradient, the Soret effect [1]. Experiments have measured the transport of rigid particles and DNA in liquids along a temperature gradient [2–4]. They have stimulated theoretical studies of hydrodynamic stress and surface forces in such states [5,6].

In particular, in a water solution at room temperature, a large volume fraction of the PEG (polyethylene glycol) polymer will lead to an exponential concentration of PEG, away from the hot region. It has been shown that a small concentration of microbeads accumulates then at the hot spot, thus reversing the effect present without the polymer [7]. The restoring force that brings beads back to the hot region has many origins [5,8,9], but they are all based on the presence of the PEG gradient. For rigid objects, the force is associated with a depletion zone around the object [7]. The word ''diffusiophoresis'' has been introduced to define those forces.

The main focus of this Letter is on DNA and RNA under a temperature gradient. We show, for the first time, that size separation of DNA or RNA is feasible in the presence of a PEG gradient, with a behavior similar to gel electrophoresis. We also show that short and long DNA has a very different scaling behavior. By varying the concentration of PEG, while keeping a large volume fraction $\phi_{\mathrm{PEG}} > 1\%$, a suspension of DNA or RNA of a small volume fraction positions itself at various distances from the hot spot. Those distances are a function of the DNA or RNA lengths. DNA and RNA are compressible objects, each with a radius of gyration R_g. In a PEG gradient, the change in compressibility for short DNA or RNA seems to be the driving force.

Thermal transport of biomolecules has applications for DNA amplification [10] and binding kinetics [11]. Also, such separation of biomolecules may have been used in the evolution of primitive life, particularly in deep ocean thermal vents, where temperature gradients are present. In the presence of large libraries of RNA polymers, sorting of small RNA, like ribozymes, becomes essential.

Experimental setup.—The chamber used is of 10 μm thickness to avoid convection and 500 μm width made by standard soft lithography techniques. Single channels made of polydimethylsiloxane (PDMS) elastomer (Sylgard 184, Dow Corning) closed with a glass slide base were filled with the water solution and sealed with a curing epoxy (Araldite Rapid). We used an epifluorescence microscope (Olympus, IX70) [Fig. 1(a)] and a 40× objective. The microscope stage was kept at room temperature ($T_\infty = 24 \pm 1\,^\circ\mathrm{C}$). To create a temperature gradient by laser heating, the condenser was replaced by a focusing system (8 mm collimator lens and objective lens 32 ×) connected to a fibered infrared laser (FOL1402PNJ, $\lambda = 1480$ nm, $P_{\mathrm{max}} = 200$ mW, Furukawa Electronics) [Fig. 1(a)]. The temperature profiles $\Delta T(r) = T(r) - T_\infty$ are shown in Fig. 1(b).

Thermophoresis of a single solute, PEG.—We used PEG conjugated with fluorescent dye (NANOCS, Rhodamine-PEG10000) dispersed in Tris *p*H7.6 buffer with a PEG volume fraction of bulk solution ϕ_{PEG} ($\phi_{\mathrm{PEG}} = 1, 2, 3, 4, 5\%$). Beyond the critical volume fraction $\phi^*_{\mathrm{PEG}} = 1.2\%$, the polymer is in a semidilute regime [12,13]. Laser heating ($\nabla T = 0.25$ K/μm, $\Delta T_{\mathrm{max}} = 5$ K) [14] expelled the polymer from the hot region [Fig. 1(c)]. The phenomenological equation for the flow J is

$$J = -D^{\mathrm{PEG}} \nabla c - c D_T^{\mathrm{PEG}} \nabla T. \quad (1)$$

D^{PEG} is PEG's diffusion coefficient, c the PEG concentration, and D_T^{PEG} its thermal diffusion coefficient. In the

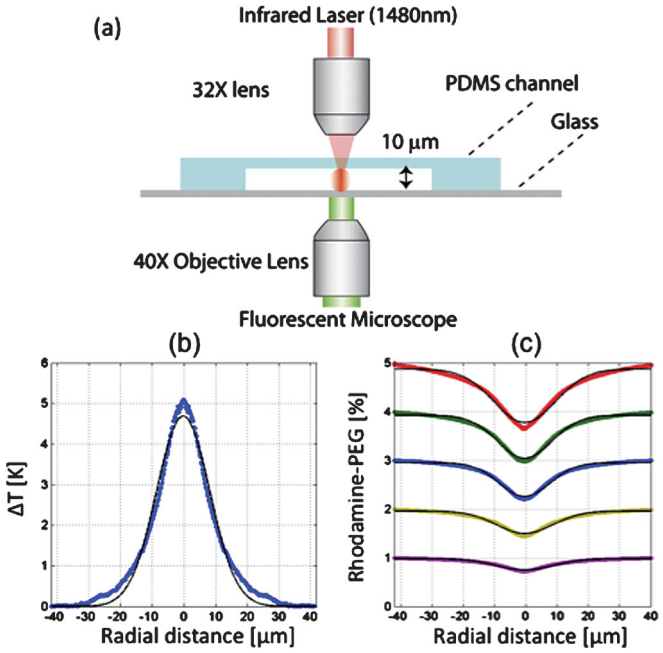

FIG. 1 (color). (a) Experimental setup. (b) Visualization of the temperature gradient. A fluorescent dye [2′,7′-bis-(2-carboxyethyl)-5-(6)-carboxyfluorescein at 1 mM concentration] was used as a temperature reporter. The fluorescence intensity map is used to determine the radial temperature profile $\Delta T(r)$. The temperature gradient curve fits a Gaussian distribution (black line). (c) PEG profiles for various initial dilutions (1%–5%). Volume fraction profiles $\phi_{\mathrm{PEG}}(r)$ are deduced from the fluorescence intensity of Rhodamine-PEG. Black lines are fitted curves using $\phi_{\mathrm{PEG}}(r) = \phi_\infty \exp[-S_T^{\mathrm{PEG}} \Delta T(r)]$.

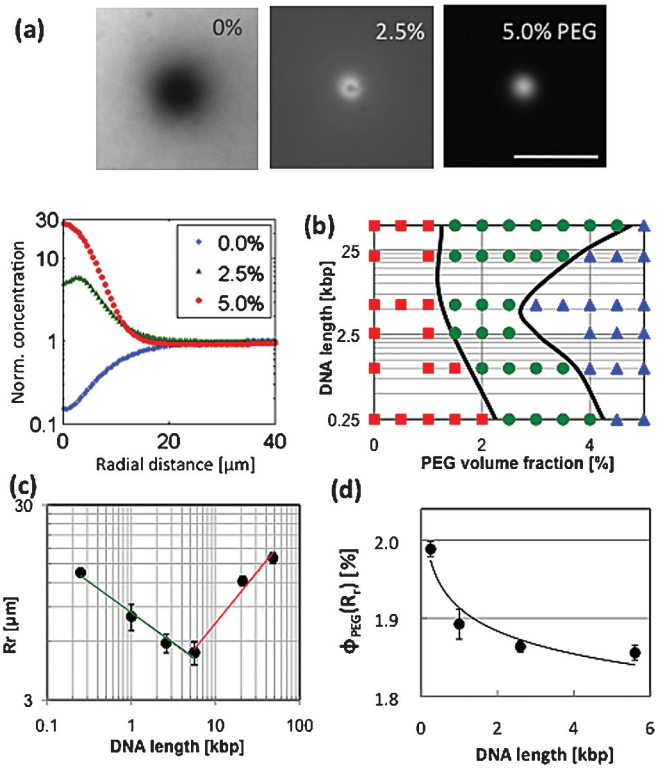

FIG. 2 (color). (a) Thermophoresis of 5.6 kbp DNA in PEG solutions. Depletion, localization, and accumulation were observed. Scale bar: 35 μm. The plot presents normalized DNA concentration vs radial distance. (b) Phase diagram of depletion (red square), ringlike localization (green circle), and accumulation (blue triangle) for DNA. (c) Ring radius R_r as a function of DNA length in 2.5% PEG solution. (d) PEG volume fraction $\phi_{\mathrm{PEG}}(R_r)$ at the peak of localization radius R_r plotted vs DNA length while ϕ_{PEG} of the bulk solution is 2.5%.

steady state ($J = 0$), $c(r) = c_\infty \exp[-S_T^{\mathrm{PEG}} \Delta T(r)]$ with the Soret coefficient $S_T^{\mathrm{PEG}} \equiv D_T^{\mathrm{PEG}}/D^{\mathrm{PEG}}$ and c_∞ the PEG concentration at the infinity. We fitted the profiles of PEG volume fraction $\phi_{\mathrm{PEG}}(r) = c(r)/\rho$ starting from different initial ϕ_{PEG} [Fig. 1(c)] [15,16]. An exponential fit with $\Delta T(r)$ deduced from Fig. 1(b) gives $S_T^{\mathrm{PEG}} = 0.064 \pm 0.002\ \mathrm{K}^{-1}$ [17]. Similar measurements for fluorescent polystyrene beads, DNA, and RNA in buffer give $S_T^{\mathrm{beads}} = 4.6 \pm 0.1\ \mathrm{K}^{-1}$ (0.5 μm beads), $S_T^{\mathrm{DNA}} = 0.38 \pm 0.05\ \mathrm{K}^{-1}$ (5.6 kbp linear DNA), and $S_T^{\mathrm{RNA}} = 0.13 \pm 0.03\ \mathrm{K}^{-1}$ (3.0 kb RNA).

Thermal separation of DNA and RNA in a PEG solution.—We first analyzed thermophoresis of double-strand DNA of a small volume fraction ($\phi_{\mathrm{DNA}} = 0.01\%$) in the presence of nonfluorescent PEG10000 of a large volume fraction. DNA was visualized by SYBR green [15]. We observed a new behavior: ringlike localization of 5.6 kbp DNA within $\phi_{\mathrm{PEG}} = 1.5\%$–$2.5\%$ [Fig. 2(a)]. In addition, DNA concentrated in the center above $\phi_{\mathrm{PEG}} > 3.0\%$, while it is depleted from the heated region for ϕ_{PEG} below 1.0% [Fig. 2(a)]. The phase diagram of DNA lengths N vs PEG volume fractions is presented in Fig. 2(b). Each dot corresponds to a measured value. Intriguingly, for long DNA such as 48.5 kbp lambda DNA, the regime of ring localization is expanded to 4.5% PEG. This is not related to a change in D_T^{DNA}, which remains almost constant ($D_T^{\mathrm{DNA}} = 1.1\ \mu\mathrm{m}^2\,\mathrm{s}^{-1}\,\mathrm{K}^{-1}$ for 5.6 kbp DNA, and $D_T^{\mathrm{DNA}} \propto N^{-0.08}$) [18,19].

From 250 bp up to 48.5 kbp, a ringlike localization was observed at the intermediate PEG volume fraction of 2.5% [Fig. 2(b)] [20]. We thus measured the ring radius R_r as a function of DNA size [Fig. 2(c)] [21]. It scales as $R_r \propto N^{-0.3}$ below 5.6 kbp [Fig. 2(c), green line]. Such scaling is close to gel electrophoresis of DNA [22]. But for long DNA above 5.6 kbp, the scaling reverses and follows $R_r \propto N^{0.5}$ [Fig. 2(c), red line]. This surprising reversal might be caused by the unfolding of long DNA chains induced by strong drag forces of the PEG polymer. It might be similar to the reptation mechanism observed in electrophoresis for large DNA [23].

We also measured how $\phi_{\mathrm{PEG}}(R_r)$ at the peak of the fluorescent ring varies with DNA length [21]. For short DNA, the dependence of $\phi_{\mathrm{PEG}}(R_r)$ on DNA length N is a monotonically decreasing nonlinear function [Fig. 2(d)].

The same experiment performed on RNA labeled with Alexa Fluor-UTP shows that RNA of various sizes from 0.1 to 3.0 kb diluted in PEG solutions exhibited also the 3 regimes (depletion, localization, and accumulation), as

ϕ_{PEG} was increased [Fig. 3(a)] [24]. The measured value of $\phi_{\mathrm{PEG}}(R_r)$ at the peak decreases as RNA becomes longer [Fig. 3(b)].

It motivated us to separate two RNA of different sizes. We mixed two RNA polymers ($\phi_{\mathrm{RNA}} = 0.01\%$ 3 kb RNA labeled by Alexa-546-UTP and $\phi_{\mathrm{RNA}} = 0.05\%$ 0.1 kb transfer RNA labeled by Ribo-Green) in a PEG solution ($\phi_{\mathrm{PEG}} = 2.0\%$). In a temperature gradient, the visualization showed that long RNA accumulated at the center while short RNA localized to form a ring [Fig. 3(c)].

We can also separate RNA from DNA. We mixed 3 kb RNA labeled with Alexa-488-UTP and 250 bp DNA labeled by carboxytetramethylrhodamine in 3.0% PEG solution. The segregated localization of RNA from DNA was observed [Fig. 3(d)]. It is thus possible to separate 3 different polymers (DNA, RNA, and PEG) in a temperature gradient.

Thermal separation of colloidal beads.—We then examined ringlike localization of a dilute suspension of carboxylated fluorescent polystyrene beads ($\phi_{\mathrm{beads}} = 0.1\%$, 0.5 μm diameter, Molecular probes F8893). Ringlike localization of beads was observed at intermediate volume fractions $1.5\% \leq \phi_{\mathrm{PEG}} \leq 2.5\%$ [Fig. 4(a)]. The plot of $\phi_{\mathrm{PEG}}(R_r)$ monotonically decreases as a function of bead size d, following approximately $\phi_{\mathrm{PEG}}(R_r) \propto d^{-0.3}$ [Fig. 4(b), solid curve]. We mixed beads having two different diameters (red, 0.5 μm $\phi_{\mathrm{beads}} = 0.05\%$; green, 0.1 μm $\phi_{\mathrm{beads}} = 0.001\%$) with PEG. Upon local laser heating, for $\phi_{\mathrm{PEG}} = 2.5\%$, big beads accumulate while small beads form a ring [Fig. 4(c)] showing size separation.

Theoretical interpretation of localization.—To capture the mechanism of ringlike localization, let us consider a theoretical model of diffusiophoresis for beads [7]. The osmotic pressure gradient of PEG occurring within the depletion layer at the surface of beads results in shear stress that makes beads migrate against the Soret effect [5,7,8,25]. By taking into account diffusiophoresis with the no-slip condition, the flux of beads J obeys

$$J = c^b u - D\nabla c^b - c^b D_T \nabla T, \tag{2}$$

where c^b, D, and D_T are the bead concentration, diffusion coefficient, and thermal diffusion coefficient, respectively. The first term in Eq. (2) takes into account the diffusiophoresis under the PEG concentration gradient, with the diffusiophoretic velocity of beads $u(r) \approx \frac{k_B T}{3\eta} S_T^{\mathrm{PEG}} \lambda^2 c_{\mathrm{PEG}}(r) \nabla T(r)$, where λ is the depletion depth of PEG from the bead surface, η is the viscosity of the solution, k_B is the Boltzmann constant, and $c_{\mathrm{PEG}}(r)$ is the local concentration of PEG [7,8]. $c_{\mathrm{PEG}}(r)$ follows $\rho\phi_{\mathrm{PEG}}(r) = \rho\phi_\infty \exp[-S_T^{\mathrm{PEG}}\Delta T(r)]$, where ϕ_∞ is the PEG volume fraction at infinity. Solving Eq. (2) in a steady state $J = 0$, we obtain the distribution of c^b as $c^b(r) = c^b_\infty \exp\{-S_T^{\mathrm{beads}}\Delta T(r) + \rho V[\phi_\infty - \phi_{\mathrm{PEG}}(r)]\}$ with $V = \pi\lambda^2 d$, where d is the bead diameter and c^b_∞ the bead concentration at the infinity. Because $\Delta T(r)$ varies in space, $\ln[c^b(r)/c^b_\infty]$ has a local maximum point at $\Delta T_C = \frac{1}{S_T^{\mathrm{PEG}}} \ln \frac{\rho\phi_\infty V S_T^{\mathrm{PEG}}}{S_T^{\mathrm{beads}}}$. Thus ringlike localization of beads occurs

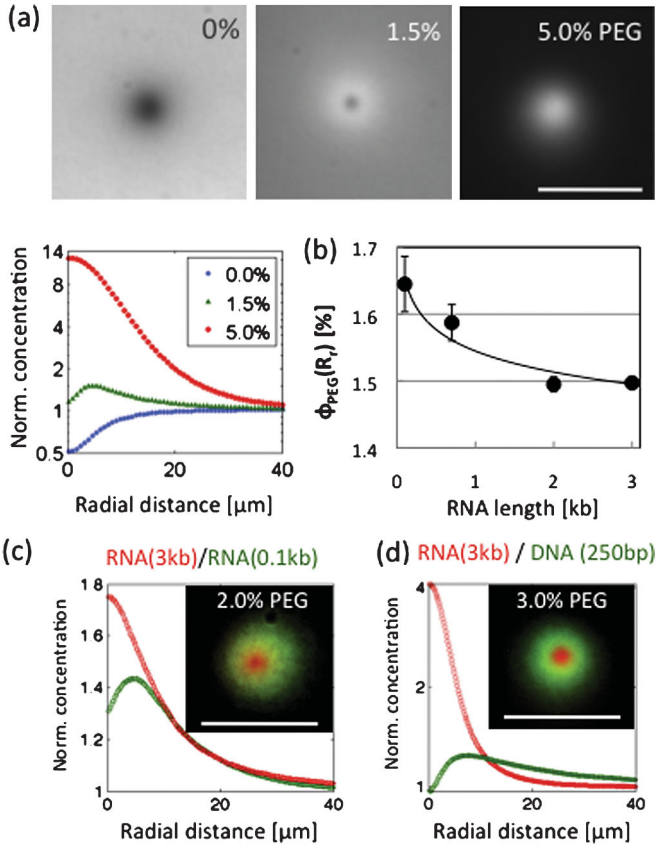

FIG. 3 (color). (a) Thermophoresis of 3.0 kb RNA in PEG solutions. (b) PEG volume fraction $\phi_{\mathrm{PEG}}(R_r)$ vs RNA length. ϕ_{PEG} of the bulk solution is 2.0%. (c) Separation of two RNA polymers (red, 3.0 kb; green, 0.1 kb) in 2.0% PEG. (d) Separation of RNA (red, 3.0 kb) and DNA (green, 250 bp) in 3.0% PEG. Scale bar: 35 μm.

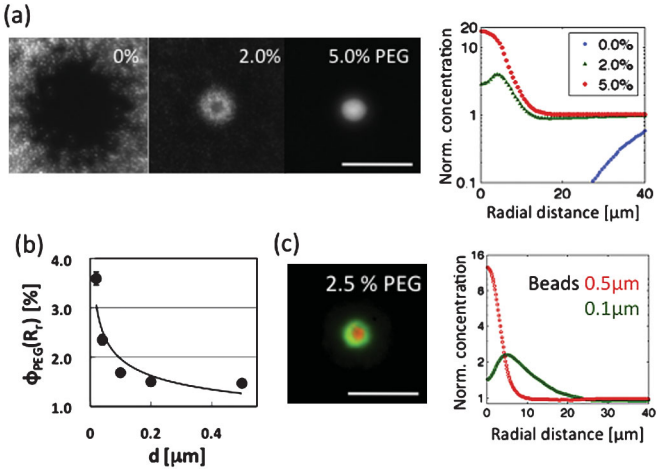

FIG. 4 (color). (a) Thermophoresis of 0.5 μm beads in PEG solutions. (b) $\phi_{\mathrm{PEG}}(R_r)$ vs bead diameter d. ϕ_{PEG} of bulk solutions that are close to the onset of localization are 2.0% for 0.1, 0.2, and 0.5 μm, 3.0% for 40 nm, and 4.5% for 20 nm beads. (c) Separation of 0.5 (red) and 0.1 μm (green) beads in 2.5% PEG. Scale bar: 35 μm.

at $\phi_{\mathrm{PEG}}(R_r) = \phi_\infty \exp[-S_T^{\mathrm{PEG}} \Delta T_C]$. We note that further investigations, e.g., the change of viscosity due to PEG gradients, would be required to understand the nonlinear relation between $\phi_{\mathrm{PEG}}(R_r)$ and d that makes two different sized beads separable.

On the other hand, DNA and RNA do not have a solid interface and are compressible molecules. The gradient of compression of these polymers could be relevant to the generation of a restoring entropic force in gradients of temperature and PEG concentration [26]. A full description is beyond the scope of this Letter.

Conclusion.—In this study, we used PEG as the polymer of a large volume fraction imposing separation of solutes. The generation of nonequilibrium entropic forces by polymer gradients is a general phenomenon. Our observation is the first demonstration of how a polymer migrates in the mesh of another polymer under a temperature gradient. We also found that small RNA can accumulate by the gradient of another RNA of a large volume fraction in a temperature gradient [27]. This might be relevant for the origin of life scenario near a thermal vent. This comes in addition to a past experiment where DNA accumulation and amplification were feasible under thermal convection [10]. Furthermore, the size-dependent localization of polymer mixtures offers new perspectives for nonequilibrium polymer dynamics. Finally, a one-dimensional shallow gradient will realize a better separation resolution [28], and the integration within a microfluidic device may offer novel applications [25,29].

We thank J. F. Joanny, H. Wada, N. Yoshinaga, J. Merrin, and P. Kumar for useful comments. Y. T. M. was supported by JSPS and M. J.&H. Kravis and A. L. by NSF Grant No. PHY-0848815.

[1] C. Ludwig and S.-B. Akad. Wiss. Wien, Nature (London) **20**, 539 (1856); C. Soret, Arch. Sci. **3**, 48 (1879); D. Braun and A. Libchaber, Phys. Rev. Lett. **89**, 188103 (2002).
[2] S. Duhr and D. Braun, Phys. Rev. Lett. **96**, 168301 (2006); Proc. Natl. Acad. Sci. U.S.A. **103**, 19 678 (2006); F. M. Weinert, J. A. Kraus, T. Franosch, and D. Braun, Phys. Rev. Lett. **100**, 164501 (2008).
[3] L. H. Thamdrup, N. B. Larsen, and A. Kristensen, Nano Lett. **10**, 826 (2010).
[4] Y. Lamhot *et al.*, Phys. Rev. Lett. **103**, 264503 (2009); Y. Lamhot, A. Barak, O. Peleg, and M. Segev, Phys. Rev. Lett. **105**, 163906 (2010).
[5] F. Jülicher and J. Prost, Eur. Phys. J. E **29**, 27 (2009).
[6] R. Piazza and A. Parola, J. Phys. Condens. Matter **20**, 153102 (2008).
[7] H. R. Jiang, H. Wada, N. Yoshinaga, and M. Sano, Phys. Rev. Lett. **102**, 208301 (2009).
[8] J. L. Anderson, Annu. Rev. Fluid Mech. **21**, 61 (1989).
[9] A. Würger, Rep. Prog. Phys. **73**, 126601 (2010).
[10] C. B. Mast and D. Braun, Phys. Rev. Lett. **104**, 188102 (2010).
[11] C. J. Wienken *et al.*, Nature Commun. **1**, 100 (2010).
[12] M. Doi and S. F. Edwards, *The Theory of Polymer Dynamics.* (Clarendon, Oxford, 1986); P. G. de Gennes, *Scaling Concepts in Polymer Physics* (Cornell University, Ithaca, 1979).
[13] V. A. Parsegian, R. P. Rand, and D. C. Rau, Methods Enzymol. **259**, 43 (1995).
[14] We visualize temperature increase by the drop of fluorescence of 2′,7′-bis-(2-carboxyethyl)-5-(6)-carboxyfluorescein. The fluorescence intensity is $-1.3\%/\mathrm{K}$ at a peripheral temperature of 24 °C.
[15] Rhodamine-PEG and SYBR green dye were sensitive to temperature as $-0.8\%/\mathrm{K}$ and $-1.0\%/\mathrm{K}$, respectively. The decrease of fluorescence was rescaled.
[16] The volume fraction ϕ_{PEG} is calculated from $\phi_{\mathrm{PEG}} = c_{\mathrm{PEG}}/\rho$ with ρ the density of PEG powder ($1.08\ \mathrm{g/cm^3}$) in the experiment and c_{PEG} its concentration.
[17] J. Chan, J. J. Popov, S. Kolisnek-Kehl, and D. G. Leaist, J. Solution Chem. **32**, 197 (2003).
[18] We estimated D of solutes (DNA, RNA, and beads) by using the time for recovery. After depletion of the solute by a great temperature gradient, the solute diffuses back as $c(r,t) = A\,\mathrm{erfc}[(r_0 - r)/\sigma(t)] + B$. We fitted this function to the fluorescent intensity profile to obtain σ and determined D by fitting $\sigma = \sqrt{4Dt}$.
[19] The fit on the density profiles of beads with Eq. (1) gives S_T. Using D measured by [18] and the expression of $S_T = D_T/D$, we obtained D_T. Typical values are $S_T^{\mathrm{DNA}} = 0.38\ \mathrm{K^{-1}}$ and $D_T^{\mathrm{DNA}} = 1.1\ \mu\mathrm{m^2\,s^{-1}\,K^{-1}}$ (5.6 kbp DNA), $S_T^{\mathrm{beads}} = 0.83\ \mathrm{K^{-1}}$ and $D_T^{\mathrm{beads}} = 3.4\ \mu\mathrm{m^2\,s^{-1}\,K^{-1}}$ (0.1 μm beads), and $S_T^{\mathrm{beads}} = 4.6\ \mathrm{K^{-1}}$ and $D_T^{\mathrm{beads}} = 3.8\ \mu\mathrm{m^2\,s^{-1}\,K^{-1}}$ (0.5 μm beads). D_T^{beads} is unaffected by the size of beads.
[20] We obtained 250 bp and 1 kbp DNA by polymerase chain reaction and 2.6 and 5.6 kbp of linear plasmids by EcoR1, and 21 kbp is a fragment of lambda DNA.
[21] The radius R_r is defined as the distance from the center of the hot region to the peak of ringlike localization. $\phi_{\mathrm{PEG}}(Rr)$ is deduced from the plot of $\phi_{\mathrm{PEG}}(r)$ in Fig. 1(c).
[22] J. L. Viovy, Rev. Mod. Phys. **72**, 813 (2000).
[23] J. Han and H. G. Craighead, Science **288**, 1026 (2000); W.-C. Liao *et al.*, Electrophoresis **31**, 2813 (2010).
[24] We obtained RNA fragments through in vitro transcription by T7 RNA polymerase. RNA was purified after the digestion of template DNA.
[25] B. Abécassis *et al.*, Nature Mater. **7**, 785 (2008); J. Palacci *et al.*, Phys. Rev. Lett. **104**, 138302 (2010); B. Abécassis *et al.*, New J. Phys. **11**, 075022 (2009).
[26] A. Grosberg (private communication).
[27] Y. T. Maeda (unpublished).
[28] H. Salman *et al.*, Phys. Rev. Lett. **97**, 118101 (2006).
[29] L. R. Huang *et al.*, Phys. Rev. Lett. **89**, 178301 (2002); G. Mahmud *et al.*, Nature Phys. **5**, 606 (2009).